

A Theoretical Study of the Mechanism of the Hydride Transfer Reaction between Alkanes and Alkenes Catalyzed by an Acidic Zeolite

M. Boronat,[†] P. Viruela,[‡] and A. Corma^{*,†}

Instituto de Tecnología Química UPV-CSIC, Universidad Politécnica de Valencia, av/ dels Tarongers s/n, 46022 Valencia, Spain, and Departament de Química Física, Universitat de València, c/ Dr. Moliner 50, 46100 Burjassot (Valencia), Spain

Received: March 13, 1998

Density functional theory has been used to study the mechanism of the hydride transfer between alkanes and alkenes catalyzed by an acidic zeolite. The $(\text{C}_3\text{H}_7\text{—H—C}_3\text{H}_7)^+$, $(t\text{-C}_4\text{H}_9\text{—H—}t\text{-C}_4\text{H}_9)^+$, and $(\text{C}_3\text{H}_7\text{—H—}t\text{-C}_4\text{H}_9)^+$ carbonium ion intermediates through which hydride transfer reactions proceed in the gas phase have been localized adsorbed on the catalyst surface, and they have been characterized, like in the gas phase, as reaction intermediates. However, they are about 25 kcal/mol less stable than separated reactants, and consequently, it will be difficult to detect them experimentally. The complete reaction path for the zeolite-catalyzed hydride transfer between propane and propene has been calculated, and it has been found that the $(\text{C}_3\text{H}_7\text{—H—C}_3\text{H}_7)^+$ carbonium ion intermediate directly decomposes into propane and propene, and not into propane and a covalent alkoxide as previously reported. The activation barrier was calculated assuming this mechanism is in very good agreement with the only available estimation of this value. It has also been shown that the geometries and energies provided by the B3PW91 and B3LYP functionals are equivalent and in very good agreement with the MP2 values and that increasing the basis set size does not significantly alter the results.

Introduction

The transformation of hydrocarbons over solid acid catalysts is a matter of great importance not only for fundamental reasons but also from the point of view of industrial processes in the field of oil refining, petrochemistry, and production of chemicals. Among the large variety of acid catalysts that have been applied to those industrial processes, zeolites are the most widely used today due to their high activity, selectivity, and thermal and hydrothermal stability.^{1,2} This, together with the fact that zeolites are crystalline solids whose structure and nature of the acid sites can be exactly determined, makes these materials very useful catalysts to carry out detailed mechanistic studies involving hydrocarbons on solid acids.

The mechanism of acid catalysis on solids such as zeolites has generally been considered to be analogous to that of homogeneous reactions in superacid media. It is then supposed that the interaction of a hydrocarbon molecule with a Bronsted acid site of the zeolite results in the formation of a carbenium ion intermediate that can undergo isomerization, β -scission, alkylation, etc., yielding a different carbenium ion intermediate. This new carbenium ion can desorb as an olefin, restoring the zeolite Bronsted acid site, or can abstract a hydride ion from an alkane reactant to give an alkane product and a carbenium ion of the reactant molecule adsorbed on the zeolite surface. Thus, the hydride transfer between alkanes and alkylcarbenium ions is the elementary step responsible for chain propagation of the acid-catalyzed transformations of hydrocarbons, and therefore it is important to understand in depth the detailed mechanism through which this reaction occurs.

The mechanism of secondary–secondary, tertiary–tertiary, and secondary–tertiary hydride transfer reactions between alkanes and alkylcarbenium ions in the gas phase has been theoretically investigated by means of traditional *ab initio*^{3,4} and density functional theory based⁴ methods, and it has been found that these ion–molecule reactions proceed through a mechanism consisting of two steps: formation of a stable tight carbonium ion intermediate having an open linear C–H–C bond and decomposition of the complex to the products without activation energy. However, when the reaction occurs on a zeolite surface, its mechanism may not be so simple. First, the initial reactants are not ionic but neutral species: two hydrocarbon molecules and the acid hydroxyl group of the zeolite Bronsted active site. It is generally supposed that carbocations are formed on these sites by proton addition either to an olefin or to a paraffin, resulting in this last case in formation of a nonclassical pentacoordinated carbonium ion which decomposes to a carbenium ion and H₂ or a smaller alkane. However, except for alkyl-substituted cyclopentenyl⁵ and indanyl⁶ cations in which the positive charge is delocalized and sterically inaccessible to framework oxygens, no free carbenium ions have been experimentally observed on the surface of acidic zeolites. Instead, a number of ¹³C NMR spectroscopic^{7–9} and quantum chemical^{10–12} studies suggest that the intermediate species in zeolite-catalyzed hydrocarbon reactions do not exist as free ions but are covalently bonded to the zeolite framework oxygens, forming stable alkoxy complexes. This means that, in order for the reaction to occur, the strong C–O bond of the stable alkoxy complex should be stretched so that some ionic character appeared in the system in order to induce the hydride transfer from the alkane, a process that would certainly require a high activation energy. Indeed, Kazansky and Van Santen¹³ have studied theoretically the mechanism of the hydride transfer between several alkanes and

* To whom correspondence should be addressed.

[†] Universidad Politécnica de Valencia.

[‡] Universitat de València.

surface alkoxides using the HF ab initio method and MP2(fc)//HF single-point calculations, and they have obtained activation energies between 47.5 and 66.5 kcal/mol.

Recently, alternative mechanisms that do not involve the formation of alkoxide intermediates have been proposed for zeolite-catalyzed monomolecular cracking of *n*-butane¹⁴ and double-bond migration in linear butene.¹⁵ In the first case, it was found that the process yields directly an alkane and an alkene. In a similar way, it could be possible that the positive character that appears in the olefin when this is being protonated by the acid hydroxyl group of a zeolite is enough to induce the hydride transfer from an alkane, this process being less energy-demanding than the breaking of a covalent alkoxy complex. Finally, it should be considered that the carbonium ion intermediates through which the hydride transfer occurs in the gas phase might not exist in the interior of the zeolitic cavities, and if they exist, their nature and stability might be different. It is then necessary to include explicitly the interaction of the organic reactants with the solid catalyst in any theoretical investigation directed to elucidate the mechanisms of solid acid-catalyzed reactions.

We present here a complete quantum chemical study of the mechanism of the hydride transfer between propene and propane catalyzed by an acidic zeolite. The active site of the catalyst has been simulated by a cluster consisting of two silicon and one aluminum tetrahedra. This cluster contains both the Bronsted acid hydroxyl group and one of the neighboring basic oxygens, and consequently it can correctly model the bifunctional nature of the zeolite active sites. The reaction intermediates for the zeolite-catalyzed hydride transfer reactions between propene and isobutane and between isobutene and isobutane have also been calculated and compared with the gas-phase results.

Computational Details

All calculations in this work were performed on IBM RS/6000 and SGI Power Challenge L workstations by means of the Gaussian 94¹⁶ computer program and, except where otherwise stated, are based on density functional theory,^{17,18} a methodology that allows for inclusion of electron correlation at a much lower computational cost than traditional ab initio methods. This is especially important in theoretical studies of heterogeneous catalysis, where large systems are involved and the inclusion of electron correlation is essential to correctly describe the interactions between molecules and the catalyst surface. In relation with the performance of the different functionals available nowadays, several comparative studies¹⁹ indicate that the results provided by hybrid methods that include the Hartree–Fock exact exchange are comparable to those obtained with post-HF correlated methods such as for example MP2. The method mainly used in this work combines Becke's hybrid three-parameter exchange functional²⁰ with the gradient-corrected correlation functional of Perdew and Wang²¹ (B3PW91) and employs the standard 6-31G* basis set²² that includes d-type polarization functions on nonhydrogen atoms. To test the influence of methodology and basis set size on the calculated geometries and energies, one of the systems has been also optimized using the B3PW91 functional and the Dunning's full double- ζ basis set D95(d,p),²³ the B3LYP functional²⁴ with both the 6-31G* and the D95(d,p) basis sets, and the much more expensive ab initio MP2 method²⁵ with the 6-31G* basis set.

The geometry of both minima and transition states was fully optimized using the Bery analytical gradient method,²⁶ and the nature of all stationary points was characterized by calculat-

ing the Hessian matrix and analyzing the vibrational normal modes. The total energies were corrected with zero-point vibrational energies (ZPE) obtained from frequency calculations. Finally, single-point calculations using the ab initio second-order Moeller–Plesset perturbation theory were performed on the B3PW91/6-31G* optimized geometries (MP2//B3PW91).

When studying the mechanism of solid acid-catalyzed reactions by quantum chemical methods, the main problem is the infinite nature of the solid catalyst. To solve it, several different approaches can be used: (a) the cluster model, used in this work, in which the solid catalyst is simulated by a limited number of atoms that are cut out from the solid and treated as a molecule; (b) embedded cluster calculations, in which the cluster is embedded in a lattice of point charges that simulate the Madelung potential of the crystal; and (c) periodic calculations of perfect crystalline solids that take advantage of the translational symmetry of the crystal. Although the periodic approach seems to be the more realistic because the long-range electrostatic potential of the crystal is included and boundary effects are absent, its computational cost is really high, and at the present it is not able to perform geometry optimizations, frequency calculations, or transition-state search calculations. In contrast, the cluster approach allows for the use of high-quality basis sets, the inclusion of electron correlation, and the performance of minima and transition-state geometry optimizations and frequency calculations, and therefore it is particularly suited to describe local phenomena such as the interaction of organic molecules with catalytically active sites. One of the disadvantages of the cluster approach is that long-range electrostatic effects caused by the rest of the crystal are neglected. The embedding scheme tries to close the gap between the cluster and the periodic approaches. However, it has been shown that it usually overestimates the effect of the long-range electrostatic potential on the calculated energies, while it has no influence on the shape of the potential energy surface.^{27,28} It has also been reported²⁹ that the errors due to neglected long-range electrostatic effects in the cluster approach are not as important as errors connected with assuming fixed or only partially relaxed structures or errors related with the choice of the computational method. Therefore, we have used in this work the cluster approach, always keeping in mind that the relative energies reported represent a higher limit due to neglect of the long-range electrostatic effects.

The cluster used to simulate the active site of the zeolite consists of one aluminum and two silicon tetrahedra whose dangling bonds, which actually connect the cluster with the rest of the solid, are saturated with hydrogen atoms H₃Si–OH–AlH₂–O–SiH₃. To avoid artificial distortions that would not occur in the zeolite crystal, the heavy atoms of the cluster were always constrained to be in the same plane, this one being the only symmetry restriction used in the geometry optimizations.

Results and Discussion

The three carbonium ion intermediate complexes through which secondary–secondary, tertiary–tertiary, and secondary–tertiary hydride transfer reactions were found to proceed in the gas phase⁴ have been now localized adsorbed on the catalyst surface, and the complete mechanism for the zeolite-catalyzed hydride transfer between propane and propene has been calculated.

1. Reaction Intermediates. The optimized geometry of the most stable conformation obtained for the (C₃H₇–H–C₃H₇)⁺ carbonium ion adsorbed on the zeolite surface, structure **1**, is shown in Figure 1a, and the calculated values of the most

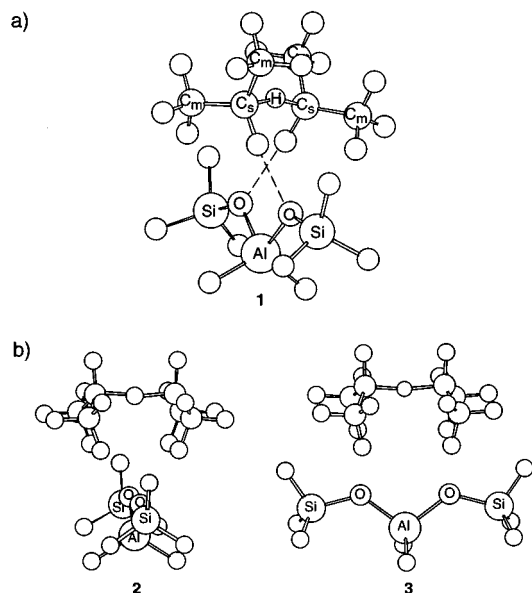


Figure 1. Optimized structure of (a) gauche and (b) cis conformations of $(\text{C}_3\text{H}_7\text{-H-C}_3\text{H}_7)^+$ carbonium ion adsorbed on a zeolite.

important geometric parameters are given in Table 1. The B3PW91/6-31G* $\text{C}_s\text{-C}_s$ and $\text{C}_s\text{-H}$ calculated bond length values of the adsorbed cation, 2.508 and 1.267 Å, respectively, are very similar to those previously obtained for the isolated system,⁴ 2.544 and 1.276 Å, respectively. The two hydrogen atoms attached to the secondary carbon atoms adopt a gauche conformation as in the gas phase, and they orientate toward the oxygen atoms of the cluster, which are at a calculated distance of less than 2.0 Å. The most important change observed in the geometry of the $(\text{C}_3\text{H}_7\text{-H-C}_3\text{H}_7)^+$ cation by adsorption on the catalyst surface corresponds to the closing of the C-H-C angle from 180° in the gas phase to 163.5°, a change which is probably caused by the interaction of the two hydrogens bonded to the secondary carbon atoms with the basic oxygens of the zeolite. The total positive charge on the organic fragment is high, +0.825e, and its distribution is also equivalent to that of the isolated carbonium ion.

Structure 1 has been characterized by analytically calculating the vibrational frequencies, and it has been found to have only one small imaginary vibrational mode of 23.6i cm^{-1} associated with the movement of the AlH_2 group out of the plane in which the heavy atoms of the cluster are constrained. It can therefore be characterized as a minimum on the PES, and it can be considered, as in the gas phase, a reaction intermediate. However, the energetics of the process in the zeolite catalyst are different from those previously obtained in the gas phase. The $(\text{C}_3\text{H}_7\text{-H-C}_3\text{H}_7)^+$ adsorbed carbonium ion is much less stable than separated reactants, which are in this case propane, propene, and the $\text{H}_3\text{Si-OH-AlH}_2\text{-O-SiH}_3$ cluster. The calculated B3PW91/6-31G* relative energy of 1, given in Table 2, is 24.0 kcal/mol and is 24.9 kcal/mol with the ZPE correction. Besides, since the $(\text{C}_3\text{H}_7\text{-H-C}_3\text{H}_7)^+$ adsorbed carbonium ion is a reaction intermediate, there must exist a transition state connecting it with the reactants and/or the reaction products, and consequently, there will be an activation barrier for the hydride transfer reaction of at least 24–25 kcal/mol.

Two other conformations higher in energy were obtained for the $(\text{C}_3\text{H}_7\text{-H-C}_3\text{H}_7)^+$ carbonium ion adsorbed on the catalyst surface (see Figure 1b). In both structures the two hydrogen atoms bonded to the secondary carbon atoms are cis, but in one of them the $\text{C}_s\text{-H-C}_s$ bond is situated perpendicular to the cluster plane (structure 2) and in the other one it is parallel

(structure 3). The $\text{C}_s\text{-C}_s$ and $\text{C}_s\text{-H}$ bond lengths and the $\text{C}_s\text{-H-C}_s$ angle calculated for these two structures are equivalent and very similar to those obtained for the cis conformer of the isolated $(\text{C}_3\text{H}_7\text{-H-C}_3\text{H}_7)^+$ cation at the same level of theory. But while the energy difference between the gauche and the cis conformers in the gas phase is only 0.5 kcal/mol, it can be observed in Table 2 that structures 2 and 3 are about 6 and 8 kcal/mol, respectively, higher in energy than the gauche conformer 1. One of the reasons that explains these energy differences is that the carbonium ions are bonded to the catalyst surface by Coulombic interactions and also by hydrogen interactions with the oxygens of the cluster. And the stabilizing interactions existing between the hydrogen atoms of the methyl groups of the cis conformers and the oxygen atoms of the cluster are weaker than those existing in the gauche conformer, which involve the more positively charged hydrogen atoms bonded to the carbon atoms of the $\text{C}_s\text{-H-C}_s$ bridge. The weaker character of the hydrogen interactions existing in the cis conformers is reflected in longer O-H distances, which are 1.96 Å in 1, 2.15 Å in 2, and 2.26 Å in 3. The nature of the two cis $(\text{C}_3\text{H}_7\text{-H-C}_3\text{H}_7)^+$ adsorbed carbonium ions has been characterized by frequency calculations. Three small imaginary vibration modes have been obtained for each system, but since they are associated either to breaking of the symmetry plane in which the heavy atoms of the cluster are constrained or to rotation of the hydrogen terminations of the silicon atoms, both structures can be characterized as minima on the potential energy surface.

To test the influence of the methodology used on the results obtained, the geometry of structure 1 was completely reoptimized at the density functional B3PW91/D95(d,p), B3LYP/6-31G*, and B3LYP/D95(d,p) levels and at the much more expensive ab initio MP2/6-31G* level. The MP2/6-31G* calculated $\text{C}_s\text{-C}_s$ and $\text{C}_s\text{-H}$ bond lengths, 2.396 and 1.242 Å, respectively, are slightly shorter than those obtained with the B3PW91/6-31G* method and the $\text{C}_s\text{-H-C}_s$ angle value is about 15° smaller (see Figure 1 and Table 1), but the conformation of the $(\text{C}_3\text{H}_7\text{-H-C}_3\text{H}_7)^+$ fragment and its orientation and distance from the cluster are equivalent at both theoretical levels. The differences in geometry caused by changing either the functional (B3LYP instead of B3PW91) or the basis set (D95(d,p) instead of 6-31G*) are still less important, and the results provided by all these methods can be considered equivalent. The same can be said about the relative energies summarized in Table 1. The MP2/6-31G* calculated value, 22.0 kcal/mol, is equivalent to that obtained by performing a single-point calculation with the MP2 method on the B3PW91 optimized geometry, 22.6 kcal/mol, and very similar too to the B3PW91/6-31G* and B3LYP/6-31G* calculated values, 24.0 and 23.4 kcal/mol, respectively. The increase in the basis set size slightly destabilizes the carbonium ion, and the relative energies calculated using the D95(d,p) basis set are about 26 kcal/mol. Consequently, the cheaper B3PW91/6-31G* method has been used in the rest of the study, and only single-point calculations of the energy have been performed at the MP2/6-31G**/B3PW91/6-31G* level.

The optimized geometries of the $(t\text{-C}_4\text{H}_9\text{-H-}t\text{-C}_4\text{H}_9)^+$ (structure 4) and $(\text{C}_3\text{H}_7\text{-H-}t\text{-C}_4\text{H}_9)^+$ (structure 5) carbonium ions adsorbed on the zeolite surface are shown in Figure 2. It can be seen that when these two carbonium ions adsorb on the catalyst, they adopt a cis conformation in order to avoid steric repulsions between the methyl groups of the cation and the atoms of the catalyst. Two orientations were found for the $(t\text{-C}_4\text{H}_9\text{-H-}t\text{-C}_4\text{H}_9)^+$ adsorbed carbonium ion. In one of them

TABLE 1: Optimized Parameters^{a,b} (Distances in angstroms and Angles in degrees) and Relative Energies^c (in kcal/mol) of Structure 1 Calculated at Different Theoretical Levels

	B3PW91/6-31G*	B3PW91/D95(d,p)	B3LYP/6-31G*	B3LYP/D95(d,p)	MP2/6-31G*
$r(\text{C}_s\text{-H})$	1.267 (1.276)	1.263	1.273	1.266	1.242
$r(\text{C}_s\text{-C}_s)$	2.508 (2.544)	2.472	2.527	2.504	2.396
$r(\text{C}_s\text{-C}_m)$	1.495 (1.496)	1.499	1.500	1.505	1.500
	1.500	1.504	1.504	1.509	1.505
$a(\text{C}_s\text{-H-C}_s)$	163.5 (180.0)	156.2	166.0	163.1	149.4
$r(\text{C}_s\text{-O})$	3.029	3.027	3.043	3.040	3.020
$r(\text{H-O})$	1.964	1.949	1.987	1.976	1.942
E_{rel}^d	24.0 (24.9)	26.6	23.4 (24.2)	26.1	22.0

^a See Figure 1a. ^b The values in parentheses at the B3PW91/6-31G* level correspond to the isolated carbonium ion. ^c Calculated as the difference between the total energy of the adsorbed cation and the sum of the energies of propane + propene + the cluster. ^d The values in parentheses include the zero-point vibrational energy correction.

TABLE 2: Relative Energies^a (in kcal/mol) of All Structures Studied in This Work

structure	B3PW91/6-31G*	+ZPE	MP2//B3PW91
1	24.0	24.9	22.6
2	30.0	30.6	29.3
3	32.4	33.1	31.7
4	25.8	26.1	21.1
5	27.7	28.3	26.2
6	27.4	27.6	29.2

^a Calculated as the difference between the total energy of the adsorbed cation and the sum of the energies of the corresponding alkane + alkene + cluster.

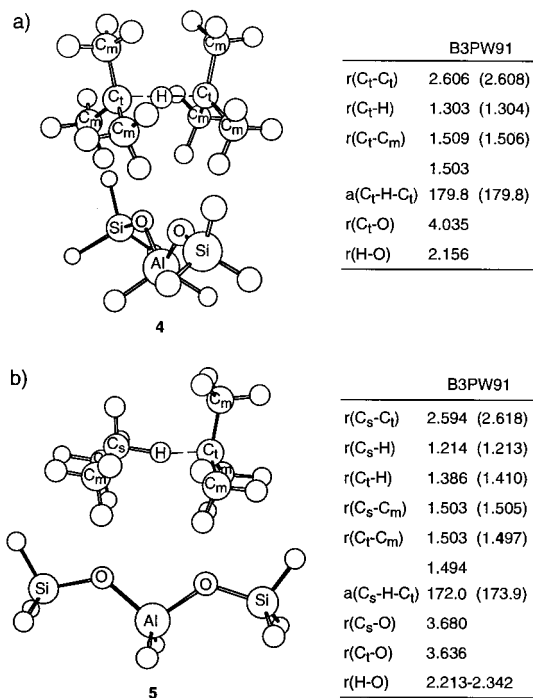


Figure 2. Optimized structure of (a) $(t\text{-C}_4\text{H}_9\text{-H-}t\text{-C}_4\text{H}_9)^+$ and (b) $(\text{C}_3\text{H}_7\text{-H-}t\text{-C}_4\text{H}_9)^+$ carbonium ions adsorbed on a zeolite. Distances in angstroms and angles in degrees. The values in parentheses correspond to the isolated carbonium ions.

(structure 4) the $\text{C}_1\text{-H-C}_1$ axis is perpendicular to the cluster plane, and in the other one, which is 2.3 kcal/mol less stable, the $\text{C}_1\text{-H-C}_1$ axis and the cluster are parallel. However, only the parallel orientation was localized for the $(\text{C}_3\text{H}_7\text{-H-}t\text{-C}_4\text{H}_9)^+$ carbonium ion (structure 5), because when we tried to optimize the geometry of the perpendicular orientation, the system decomposed into propane and isobutene adsorbed on the neutral $\text{H}_3\text{Si-OH-AlH}_2\text{-O-SiH}_3$ cluster. The optimized geometric parameters of the organic fragments of structures 4 and 5 are equivalent to those calculated for the isolated systems at the

same level of theory, given in parentheses in Figure 2. The total positive charge on these fragments is close to unity ($+0.820e$ in 4 and $+0.856e$ in 5), and its distribution is also equivalent to that of the isolated carbonium ions.

The $(t\text{-C}_4\text{H}_9\text{-H-}t\text{-C}_4\text{H}_9)^+$ and $(\text{C}_3\text{H}_7\text{-H-}t\text{-C}_4\text{H}_9)^+$ carbonium ions are bonded to the zeolite surface by Coulombic interactions and by four stabilizing interactions between the hydrogen atoms of the methyl groups and the oxygen atoms of the cluster. These interactions are weak, as reflected in the O-H distances of 2.2–2.3 Å, and consequently the two cations are relatively separated from the catalyst surface, the $\text{C}_1\text{-O}$ calculated distance in 4 being 4.035 Å and the $\text{C}_s\text{-O}$ and $\text{C}_1\text{-O}$ distances in 5 being 3.680 and 3.636 Å, respectively.

The relative energies with respect to separated reactants, which are isobutene + isobutane + the cluster for structure 4 and propene + isobutane + the cluster for structure 5, are listed in Table 2. The B3PW91/6-31G* calculated values for the $(t\text{-C}_4\text{H}_9\text{-H-}t\text{-C}_4\text{H}_9)^+$ adsorbed carbonium ion, 25.8 and 26.1 kcal/mol with the ZPE correction, and for the $(\text{C}_3\text{H}_7\text{-H-}t\text{-C}_4\text{H}_9)^+$ adsorbed cation, 27.7 and 28.3 kcal/mol with the ZPE correction, are similar to the values obtained for structure 1. The MP2-(fu)/6-31G* single-point calculations yield similar results, structure 4 being slightly more stabilized than the other two. Three (56.2i, 54.0i, and 37.8 i cm^{-1}) and two (47.3i and 20.9i cm^{-1}) imaginary vibration modes were obtained from the frequency calculations performed for structures 4 and 5, respectively, but since they are small in magnitude and related either to the constraints imposed on the cluster or to the hydrogen terminations of Si and Al, both adsorbed cations can be characterized as minima on their potential energy surfaces.

It can therefore be concluded that the carbonium ion intermediates through which the hydride transfer occurs in the gas phase also exist as reaction intermediates when the process is catalyzed by a zeolite, although they are energetically less stable than separated reactants, and consequently they will be difficult to detect experimentally. It's important to note that these results are different from those previously reported by Kazansky and Van Santen,¹³ who, using the $\text{H}_2\text{OAl}(\text{OH})_3$ cluster, C_2 symmetry, and the HF/6-31G* method, found the $(\text{C}_3\text{H}_7\text{-H-C}_3\text{H}_7)^+$ and $(t\text{-C}_4\text{H}_9\text{-H-}t\text{-C}_4\text{H}_9)^+$ adsorbed carbonium ions to be transition states that collapse to surface alkoxides and free paraffins.

2. Reaction Path. To obtain the complete mechanism for the zeolite-catalyzed propane-propene hydride transfer reaction, we have taken the $\text{C}_s\text{-C}_s$ distance in structure 1 as the reaction coordinate and we have performed a series of geometry optimizations in which this distance has been slowly varied from 2.51 to 3.00 Å. In each calculation the $\text{C}_s\text{-C}_s$ distance has been held fixed, and all other parameters except for the dihedral angles of the heavy atoms of the cluster have been allowed to

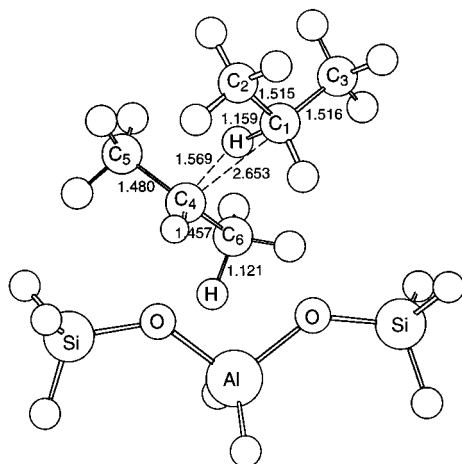


Figure 3. B3PW91/6-31G* optimized structure of the transition state for the zeolite catalyzed hydride transfer between propane and propene. Distances in angstroms and angles in degrees.

fully optimize. It has been found that as the C_5-C_6 distance increases, the central hydrogen atom moves toward one of the secondary carbon atoms, forming a propane molecule, while the other C_3 fragment orientates in such a way that one of the hydrogen atoms of a methyl group starts being transferred to the cluster, yielding a propene molecule adsorbed on the zeolite surface.

The optimized geometry of the calculated transition state for the process, structure **6**, is shown in Figure 3. The C_1-C_4 distance, 2.654 Å, is only slightly longer than in the $(C_3H_7-H-C_3H_7)^+$ intermediate **1**, 2.508 Å, but the central hydrogen atom is much closer to C_1 (1.159 Å) than to C_4 (1.569 Å). The C_1-C_2 and C_1-C_3 bond length values are similar to those calculated for isolated propane at the same level of theory, 1.527 Å, and the fragment as a whole resembles a propane molecule with a stretched C-H bond. In the other fragment the C_4-C_5 distance, 1.480 Å, is somewhat longer than the C_4-C_6 one, 1.457 Å, and one of the C_6-H bonds is slightly stretched (1.121 Å). This geometry agrees well with the obtained reaction path that involves donation of a proton from C_6 to the cluster and consequent formation of a double bond between C_4 and C_6 . The Mulliken population analysis indicates that transition state **6** is highly ionic, the total positive charge on the "propane" fragment (+0.252e) being lower than that on the "propyl" fragment (+0.532e).

Structure **6** has been characterized by a frequency calculation, and only one imaginary vibration mode of 130.8i cm^{-1} has been obtained. The reaction coordinate associated with this imaginary mode is mainly related to the movement of the central hydrogen atom toward C_1 and to the stretching of one C_6-H bond, but it also involves contributions from all carbon atoms, from the other hydrogens bonded to C_6 , and from one of the hydrogen terminations of the Al atom. By following this reaction coordinate in one sense, the $(C_3H_7-H-C_3H_7)^+$ carbonium ion intermediate **1** is reached, and by following it in the opposite sense the system decomposes into propane and propene. Due to the small size of the cluster used, the proton that is transferred from C_6 to the zeolite seems to move toward one of the hydrogen terminations of the Al atom. However, in a real zeolite, where every Al atom is bonded to four O atoms, this proton would be transferred to a SiOAl bridge, restoring the Brønsted acid site. Thus, according to these results, the zeolite-catalyzed hydride transfer reaction does not involve the formation of covalent alkoxide intermediates as proposed by Kazansky et al. We have found that this process occurs through formation

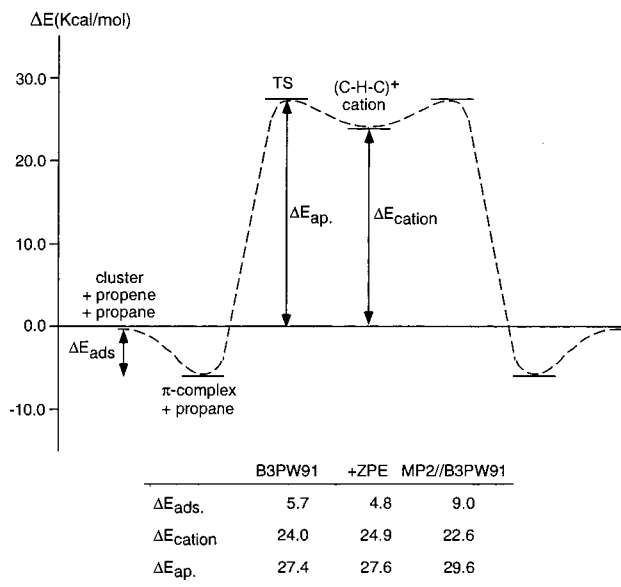


Figure 4. Calculated energy profile for the zeolite-catalyzed hydride transfer between propane and propene.

of adsorbed carbonium ion intermediates similar to those obtained in the gas phase, which decompose yielding directly an alkane and an adsorbed alkene.

Figure 4 shows the calculated energy profile for the complete process. The apparent activation energy, calculated as the energy difference between transition state **6** and the sum of the energies of propene, propane, and the cluster, is 27.4 and 27.6 kcal/mol with the ZPE correction. When the adsorption energy of propene is considered, the real activation energy is somewhat higher, 33.1 and 32.4 kcal/mol with the ZPE correction, and the same trend is observed at the MP2/6-31G**//B3PW91/6-31G* level. The energy difference between transition state **6** and structure **1** is small (3.4, 2.7, and 7.0 kcal/mol at the B3PW91/6-31G*, B3PW91/6-31G*+ZPE, and MP2/6-31G**//B3PW91/6-31G* levels, respectively), and consequently the $(C_3H_7-H-C_3H_7)^+$ adsorbed carbonium ion intermediate will be difficult to observe experimentally.

Although there are no available direct experimental data of the activation energy of hydride transfer reactions in zeolites, an estimation of this value of about 30 kcal/mol was made from the modeling of kinetics of isobutane cracking.³⁰ It can be observed that there is a very good agreement between this estimation and our theoretical results. Finally, it is important to note that the activation energy of 47.5 kcal/mol obtained by Kazansky et al.¹³ at the MP2/6-31++G**//HF/6-31G* level is comparable to the B3PW91/6-31G* value of 43.0 kcal/mol obtained by us for the energy difference between the adsorbed $(C_3H_7-H-C_3H_7)^+$ carbonium ion **1** and the sum of the energies of propane and the covalent propyl-alkoxide.

Conclusions

The mechanism of the zeolite-catalyzed hydride transfer reaction between alkanes and alkenes has been theoretically investigated by means of density functional theory, and the following conclusions have been obtained.

First, the $(C_3H_7-H-C_3H_7)^+$, $(t-C_4H_9-H-t-C_4H_9)^+$, and $(C_3H_7-H-t-C_4H_9)^+$ carbonium ion intermediates through which secondary-secondary, tertiary-tertiary, and secondary-tertiary hydride transfer reactions were found to proceed in the gas phase also exist as reaction intermediates when the process is catalyzed by an acidic zeolite. The optimized geometric parameters and

the charge distributions of these three adsorbed carbonium ions are similar to those previously obtained for the isolated systems, although in some cases they adopt a different conformation in order to avoid steric repulsions between the methyl groups and the zeolite surface. These three intermediates are bonded to the catalyst surface both by Coulombic interactions and by hydrogen interactions with the oxygens of the lattice. However, they are energetically less stable than separated reactants (which are the corresponding alkane + alkene + the zeolite Brønsted active site), and consequently they will be difficult to detect experimentally.

Second, the influence of basis set size and methodology on the results has been tested by performing a series of calculations in which the B3PW91 and B3LYP functionals and the MP2 ab initio method combined with the 6-31G* and D95(d,p) basis sets were used. It has been shown that the geometries and energies calculated with the B3PW91 and B3LYP functionals are completely equivalent and in very good agreement with the MP2 values and that increasing the basis set size does not significantly alter the results obtained.

Third, the complete reaction path for the hydride transfer between propane and propene has been calculated at the B3PW91/6-31G* level, and it has been found that the $(C_3H_7-H-C_3H_7)^+$ adsorbed carbonium ion intermediate directly decomposes through transition state **6** into propane and propene. No covalent alkoxide intermediate is formed according to this mechanism, and therefore the real activation energy necessary for the reaction to occur is not as high as if a strong covalent C–O bond had to be broken, in which case the activation barrier would be about 13 kcal/mol higher.

Acknowledgment. The authors thank the Centre de Informàtica and Departament de Química Física, University of Valencia, for computing facilities. They thank C.I.C.Y.T. (Project MAT 94-0359) and Conselleria de Cultura, Educació i Ciència de la Generalitat Valenciana, for financial support. M.B. thanks Conselleria de Cultura, Educació i Ciència de la Generalitat Valenciana, for a personal grant.

References and Notes

- (1) Corma, A. *Chem. Rev.* **1995**, *95*, 559.
- (2) Wojcechowski, B. W.; Corma, A. *Catalytic Cracking: Catalysts, Chemistry and Kinetics*; Dekker: New York, 1986.
- (3) Frash, M. V.; Solkan, V. N.; Kazansky, V. B. *J. Chem. Soc., Faraday Trans.* **1997**, *93*, 515.
- (4) Boronat, M.; Viruela, P.; Corma, A. *J. Phys. Chem. B* **1997**, *101*, 10069.
- (5) Oliver, F. G.; Munson, E. J.; Haw, J. F. *J. Phys. Chem.* **1992**, *96*, 8106.
- (6) Xu, T.; Haw, J. F. *J. Am. Chem. Soc.* **1994**, *116*, 10188.
- (7) (a) Aronson, M. T.; Gorte, R. J.; Farneth, W. E.; White, D. J. *Am. Chem. Soc.* **1989**, *111*, 840. (b) Haw, J. F.; Richardson, B. R.; Oshiro, I. S.; Lazo, N. D.; Speed, J. A. *J. Am. Chem. Soc.* **1989**, *111*, 2052. (c) Lazo, N. D.; Richardson, B. R.; Schettler, P. D.; White, J. L.; Munson, E. J.; Haw, J. F. *J. Phys. Chem.* **1991**, *95*, 9420.
- (8) Malkin, V. G.; Chesnokov, V. V.; Paukshtis, E. A.; Zhidomirov, G. M. *J. Am. Chem. Soc.* **1990**, *112*, 666.
- (9) Stepanov, A. G.; Zamaraev, K. I. *Catal. Lett.* **1993**, *19*, 153.
- (10) (a) Kazansky, V. B. *Acc. Chem. Res.* **1991**, *24*, 379. (b) Senchenya, I. N.; Kazansky, V. B. *Catal. Lett.* **1991**, *8*, 317. (c) Kazansky, V. B.; Senchenya, I. N. *J. Catal.* **1989**, *119*, 108.
- (11) Viruela, P.; Zicovich-Wilson, C. M.; Corma, A. *J. Phys. Chem.* **1993**, *97*, 13713.
- (12) Rigby, A. M.; Kramer, G. J.; Van Santen, R. A. *J. Catal.* **1997**, *170*, 1.
- (13) Kazansky, V. B.; Frash, M. V.; Van Santen, R. A. *Stud. Surf. Sci. Catal.* **1997**, *105*, 2283.
- (14) Collins, S. J.; O'Malley, P. J. *Chem. Phys. Lett.* **1995**, *246*, 555.
- (15) Boronat, M.; Viruela, P.; Corma, A. *J. Phys. Chem. A* **1998**, *102*, 982.
- (16) Frisch, M. J.; Trucks, G. W.; Schlegel, H. B.; Gill, P. M. W.; Johnson, B. G.; Robb, M. A.; Cheeseman, J. R.; Keith, T.; Petersson, G. A.; Montgomery, J. A.; Raghavachari, K.; Al-Laham, M. A.; Zakrzewski, V. G.; Ortiz, J. V.; Foresman, J. B.; Cioslowski, J.; Stefanov, B. B.; Nanayakkara, A.; Challacombe, M.; Peng, C. Y.; Ayala, P. Y.; Chen, W.; Wong, M. W.; Andres, J. L.; Replogle, E. S.; Gomperts, R.; Martin, R. L.; Fox, D. J.; Binkley, J. S.; DeFrees, D. J.; Baker, J.; Stewart, J. P.; Head-Gordon, M.; Gonzalez, C.; Pople, J. A. *Gaussian 94*, Revision B.1; Gaussian: Pittsburgh, PA, 1995.
- (17) (a) Hohenberg, P.; Kohn, W. *Phys. Rev. B* **1964**, *136*, 864. (b) Kohn, W.; Sham, L. J. *Phys. Rev. A* **1965**, *140*, 1133.
- (18) (a) Parr, R. G.; Yang, W. In *Density Functional Theory of Atoms and Molecules*; Oxford University Press: New York, 1989. (b) Dreizler, R. M.; Gross, E. K. U. In *Density Functional Theory*; Springer: Berlin, 1990. (c) March, N. H. In *Electron Density Theory of Many-Electron Systems*; Academic Press: New York, 1991.
- (19) (a) Zygmunt, S. A.; Mueller, R. M.; Curtiss, L. A.; Iton, L. E. *J. Mol. Struct. (THEOCHEM)* **1998**, *430*, 9. (b) Becke, A. D. *J. Chem. Phys.* **1996**, *104*, 1040. (c) Boronat, M.; Viruela, P.; Corma, A. *J. Phys. Chem.* **1996**, *100*, 16514. (d) Bauschlicher, C. W., Jr. *Chem. Phys. Lett.* **1995**, *246*, 40. (e) Baker, J.; Muir, M.; Andzelm, J. *J. Chem. Phys.* **1995**, *102*, 2063.
- (20) Becke, A. D. *J. Chem. Phys.* **1993**, *98*, 5648.
- (21) Perdew, J. P.; Wang, Y. *Phys. Rev. B* **1992**, *45*, 13244.
- (22) Hariharan, P. C.; Pople, J. A. *Chem. Phys. Lett.* **1972**, *16*, 217.
- (23) Dunning, T. H., Jr.; Hay, P. J. In *Modern Theoretical Chemistry*; Schaefer III, H. F., Ed.; Plenum: New York, 1976; pp 1–28.
- (24) Lee, C.; Yang, W.; Parr, R. G. *Phys. Rev. B* **1988**, *37*, 785.
- (25) (a) Moeller, C.; Plesset, M. S. *Phys. Rev.* **1934**, *46*, 618. (b) Binkley, J. S.; Pople, J. A. *Int. J. Quantum Chem.* **1975**, *9*, 229.
- (26) Schlegel, H. B. *J. Comput. Chem.* **1982**, *3*, 214.
- (27) Greatbanks, S. P.; Hillier, I. H.; Burton, N. A.; Sherwood, P. J. *J. Chem. Phys.* **1996**, *105*, 3770.
- (28) Teunissen, E. H.; Jansen, A. P. J.; Van Santen, R. A.; Orlando, R.; Dovesi, R. *J. Chem. Phys.* **1994**, *101*, 5865.
- (29) Sauer, J.; Ugliengo, P.; Garrone, G.; Saunders, V. R. *Chem. Rev.* **1994**, *94*, 2095.
- (30) Yaluri, G.; Rekoske, J. E.; Aparicio, L. M.; Madon, R. J.; Dumesic, J. A. *J. Catal.* **1995**, *153*, 54.